JOURNAL OF VIROLOGY, June 2004, p. 6439–6448 Vol. 78, No. 12
0022-538X/04/$08.00+0 DOI: 10.1128/JVI.78.12.6439–6448.2004

Characterization of Two *Autographa californica* Nucleopolyhedrovirus Proteins, Ac145 and Ac150, Which Affect Oral Infectivity in a Host-Dependent Manner

Renee Lapointe,[1,2] Holly J. R. Popham,[3] Ursula Straschil,[1] David Goulding,[1] David R. O'Reilly,[1,4] and Julie A. Olszewski[1]*

Department of Biological Sciences, Imperial College, London SW7 2AZ,[1] and Syngenta, Jealotts Hill International Research Centre, Bracknell, Berks RG42 6EY,[4] United Kingdom; Natural Resources Canada, Canadian Forest Service, Laurentian Forestry Centre, Sainte-Foy, Québec, Canada G1V 4C7[2]; and Biological Control of Insects Research Laboratory, Agricultural Research Service, U.S. Department of Agriculture, Columbia, Missouri 65203[3]

Received 4 November 2003/Accepted 3 February 2004

The genome of the baculovirus *Autographa californica* nuclear polyhedrosis virus (Ac*M*NPV) contains two homologues, *orf145* and *orf150*, of the *Heliothis armigera* Entomopoxvirus (HaEPV) 11,000-kDa gene. Polyclonal antibodies raised against the Ac145 or Ac150 protein were utilized to demonstrate that they are expressed from late to very late times of infection and are within the nuclei of infected Sf-21 cells. Transmission electron microscopy coupled with immunogold labeling of Ac145 found this protein within the nucleus in areas of nucleocapsid assembly and maturation, along with some association with the enveloped bundles of virions within the developing occlusion bodies (OBs). Ac150 was found to be mainly associated with enveloped bundles of virions within OBs and also with those not yet occluded. Both Ac145 and Ac150 were found to be present in budded virus as well as OBs. Both *orf145* and *orf150* were deleted from the Ac*M*NPV genome, singly or together, and these deletion mutants were assessed for oral infectivity both in *Trichoplusia ni* and *Heliothis virescens* larvae. Deletion of Ac145 led to a small but significant drop in infectivity (sixfold) compared to wild-type (wt) Ac*M*NPV for *T. ni* but not for *H. virescens*. Deletion of Ac150 alone had no effect on infectivity of the virus for either host. However, deletion of both Ac145 and Ac150 gave a recombinant virus with a drastic (39-fold) reduction in infectivity compared to wt virus for *H. virescens*. Intrahemocoelic injection of budded virus from the double-deletion virus into *H. virescens* larvae is as infectious to this host as wt budded virus, indicating that Ac145 and Ac150 play a role in primary oral infection of Ac*M*NPV, the extent of which is host dependent.

Baculoviruses are large double-stranded DNA viruses that are specific for invertebrate hosts, mainly lepidopteran larvae, and can be found in environments where a previous epizootic has occurred. Invertebrate hosts undergo population change due to seasonal and ecological factors so that an extended period of time can occur before a permissive host is reintroduced into the environment to allow further viral transmission (reviewed by Cory et al. in reference 5). To aid their transmission to susceptible hosts, baculoviruses have evolved a biphasic life cycle in which genetically identical budded virions and occlusion-derived virions (ODV) are produced but are enveloped and packaged in different ways, making them phenotypically distinct. The ODV are occluded within a proteinaceous structure that protects them from environmental conditions such as desiccation and UV rays, providing insect-to-insect transmission (27, 30). Occlusion of viral particles to allow delayed transmission of infection has independently arisen within two other insect-infecting virus taxa: the *Entomopoxvirinae* subfamily of the *Poxviridae* and the *Cypovirus* genus of the *Reoviridae* family (15, 16, 24).

Baculoviruses are generally highly host specific, and the host range specificity is determined at multiple levels. One of the first barriers to establishing a baculovirus infection is at the midgut level. The peritrophic membrane (PM) is a sleeve-like structure that lines the gut of insects and consists of chitin, proteoglycans, and proteins such as peritrophins and insect intestinal mucins (25). The interaction of proteins with chitin fibers into a three-dimensional mesh is essential to the bidirectional trafficking of digestive enzymes and hydrolytic products as well as for protection of the midgut epithelium from toxins and pathogens that are ingested along with the food bolus. Disruption of the link between chitin and the PM proteins results in a disruption of the midgut defense system against pathogens (20, 28, 29).

The baculovirus-encoded metalloproteinase, enhancin, has been shown to assist in the oral infectivity of the *Granulovirus* (GV) genus of baculoviruses by degrading mucins in the PM (8, 13, 28). Enhancins have been identified in many GVs but are encoded by only a few members of the *Nucleopolyhedrovirus* (NPV) genus of baculoviruses, such as *Lymantria dispar M*NPV (Ld*M*NPV; NC 001973) (12), *Mamestra congregata M*NPV (NC 004117) (14), and *Choristoneura fumiferana M*NPV (accession no. AAP29820). Both Ld*M*NPV enhancin homologues were shown to contribute to the viral infectivity of its host, the gypsy moth (19).

Dall et al. (6) utilized an informatics-based study to identify other viral strategies which provide a competitive advantage for the viral infection of invertebrate hosts. This strategy was based upon the identification of gene homologs that are found among virus taxa which are phylogenetically unrelated but

* Corresponding author. Mailing address: Department of Biological Sciences, SAFB, South Kensington Campus, London SW7 2AZ, United Kingdom. Phone: 44 0 20 7594 5376. Fax: 44 0 20 7584 2056. E-mail: j.olszewski@imperial.ac.uk.

infect an overlapping host range of invertebrates. One group of viral genes identified in this manner was named the 11,000-molecular-weight (11K) genes and was identified from homologous genes that were encoded by baculoviruses and *Heliothis* (*Helicoverpa*) *armigera* entomopoxvirus (HaEPV) but not among the vertebrate-infecting members of the poxviruses (6). The 11K-like genes were predicted to produce small proteins of between 90 and 110 amino acids with hydrophobic N termini consistent with a membrane transit signal, and a core C_6 motif of conserved cysteine residues in a well-defined spacing pattern. Additionally, all lepidopteran-infecting baculoviruses sequenced to date encode one or more of the 11K gene homologues and, through phylogenetic analyses of the core C_6 motif, have been split into two viral subtypes (6).

This motif, $CX_{7\text{-}18}CX_5CX_{6\text{-}11}CX_{12}CX_{5\text{-}11}C$, where X represents any amino acid residue other than cysteine (6), is also found in nonviral proteins from the ecdysozoan clade (1), whose functions are diverse but frequently involve interaction with chitin (26). Many of these proteins, such as insect intestinal mucins, peritrophins, and chitinases, are found associated with the PM of insects and nematodes and contain multiple repeats of the C_6 motif, also referred to as the peritrophin-A domain (26).

The baculovirus *Autographa californica* NPV (Ac*M*NPV) putatively encodes two subtypes of the core C_6 motif conserved among the 11K proteins from two predicted open reading frames (ORFs), *orf145* and *orf150* (2). Ac*M*NPV and HaEPV have very different replication strategies; however, both infect their hosts via the insect gut. This observation, along with the peritrophin-A-like domains encoded within these putative proteins suggests a function at the primary infection level for these viral proteins. In this study, we characterized the temporal expression and intracellular localization of the Ac*M*NPV Ac145 and Ac150 proteins and determined the effect of knocking out both genes, individually and together, on the virulence of Ac*M*NPV for two different lepidopteran hosts.

MATERIALS AND METHODS

Cells, viruses, and insect rearing. *Spodoptera frugiperda* (Sf-21) cells and Ac*M*NPV strain L1, as well as the various mutant viruses created, were propagated and maintained as previously described (18). *Trichoplusia ni* eggs were purchased from the NERC IVEM (Oxford, United Kingdom), and *Heliothis virescens* eggs were kindly provided by Syngenta (Bracknell, United Kingdom). *T. ni* larvae were reared on a synthetic diet at 27°C (4) while *H. virescens* larvae were maintained on a synthetic diet recipe obtained from Syngenta.

Construction of bacterial expression vectors. To generate bacterial fusion proteins lacking the 22 or 30 N-terminal amino acids corresponding to the putative signal sequence domains of ORF145 and ORF150, respectively, gene fragments were PCR amplified with the primer pairs Ac145F and Ac145R or Ac150F and Ac150R (Table 1). The amplified DNAs were ligated into the BamHI and EcoRI sites of pGEX-KG (Amersham Biosciences). The constructs obtained, pGEX-AcORF145 and pGEX-AcORF150, encoded for an N-terminal fusion of glutathione *S*-transferase (GST) with a thrombin digestion site and COOH-terminal Ac*M*NPV ORF145 and ORF150, respectively.

Expression, purification of ORF145 and ORF150, and production of polyclonal antibodies. pGEX-AcORF145 and pGEX-AcORF150 were transformed in BL21 bacterial cells (Amersham Biosciences) and induced with isopropyl-β-D-thiogalactopyranoside (IPTG, 0.2 μg/ml) for 2 h at 37°C. The bacterial culture was resuspended in STE buffer (150 mM NaCl, 10 mM Tris [pH 8], 1 mM EDTA, leupeptin [1 μg/ml], pepstatin A [1 μg/ml], aprotinin [1 μg/ml] and phenylmethylsulfonyl fluoride [100 μg/ml]) with 500 μg of lysozyme/ml and incubated on ice for 15 min. The cells were lysed with the addition of 5 mM dithiothreitol and 1.5% *N*-lauroyl-sarkosine by sonication. The soluble extracts was cleared by centrifugation at 12,000 × *g* and mixed with Triton X-100 to a concentration of 4% before incubation with a glutathione-Sepharose 4B slurry (8:1; Sigma) for 1 h at 4°C. The beads were washed in phosphate-buffered saline (PBS), and the bound proteins were eluted in glutathione elution buffer for 10 min at room temperature (RT) per the manufacturer's instructions. The GST fusion proteins were dialyzed against PBS and quantified by using the Bradford assay (Bio-Rad). The purified GST fusion proteins (~100 μg) were utilized as antigens in rabbits to produce anti-Ac145 and anti-Ac150 polyclonal sera (Oswell Research Products Ltd.).

TABLE 1. Oligonucleotides used for subcloning of the ORFs for Ac145 or Ac150 or their flanking regions

Oligonucleotide	Sequence (5′–3′)
Ac145F	GCGGGATCCCATCTAAAGTGTCACAGCGA
Ac145R	GCGGAATTCTCATAGTAACAAGTTTCTA
Ac150F	GCGGGATCCGACGATGACGAATCAGACGA
Ac150R	GCGGAATTCTTAGTTTTGGTTAGCGGTAC
145UF	GCGGAGCTCTAGTAATTATTGCTTTAATA
145UR	GCGCCGCGGATTAATAAATGTATATTATTTAATTA
145DF	GCGGAATTCCGGCTCGCATGTATAGAAAC
145DR	GCGGGGCCCTCCGGGGTGGGATGGTTATAA
150UF	GCGGAGCTCCCGCCGGTGTTATTGATGGC
150UR	GCGCCGCGGGATTCGTCATCGTCACCTCT
150DF	GCGGAATTCCTAACCAAAACTAAAAATAA
150DR	GCGGGTACCCATACTAATTAATAGTGAAA

Western blot analysis. Ac*M*NPV Ac145 and Ac150 specific primary antisera (SK852 and SK854, respectively) were preadsorbed onto mock-infected Sf-21 cells (10^7) that had first been incubated on a nitrocellulose membrane for 2 h. This nitrocellulose membrane was then blocked in 1% gelatin for 2 h, and nonspecific antibodies were preadsorbed by incubating the antisera (1/5,000) in 5% milk powder in PBS-Tween (PBST) on the nitrocellulose membrane overnight. Preadsorbed antisera were collected and used for Western blot analysis. Mock-infected or infected whole-cell extracts (5×10^4 cells) were separated on 15% gels by sodium dodecyl sulfate-polyacrylamide gel electrophoresis (SDS-PAGE) and electrophoretically transferred to a Hybond-C nitrocellulose membrane (Amersham Biosciences) according to the manufacturer's instructions. For detection of Ac*M*NPV Ac145 and Ac150 proteins, the blots were blocked with dry milk at 4°C overnight, probed with a preadsorbed 1/5,000 dilution of Ac*M*NPV Ac145 or Ac150 specific polyclonal antibodies, and visualized with horseradish peroxidase-linked goat anti-rabbit (Jackson ImmunoResearch Laboratories, Inc.) secondary antibodies at a 1:10,000 dilution in 5% milk powder in PBST by using the ECL kit (Amersham Biosciences).

Immunofluorescence. Sf-21 cells, seeded onto coverslips, were infected with Ac*M*NPV at a multiplicity of infection (MOI) of 10 and incubated at 27°C. At various times postinfection, the cells were washed gently with PBS and fixed with 10% paraformaldehyde for 10 min at RT and then permeabilized in methanol for 20 min at −20°C. After being washed three times with PBST, the cells were blocked for 1 h in 1% goat serum (in PBST). Preadsorbed Ac145 and Ac150 antisera, at 1:200 and 1:100 dilutions, respectively, were incubated with the cells for 1 h. The cells were washed twice for 30 min in PBST and then incubated for 1 h in fluorescein isothiocyanate (FITC)-linked anti-rabbit secondary antibody (1/100) (Jackson ImmunoResearch Laboratories, Inc.). Cells were washed as before in PBST, followed by three 5-min washes in PBS alone, and were incubated in RNase A (200 μg/ml) for 40 min at 37°C. Following three 5-min washes in PBST, cellular DNA was stained with propidium iodide (2 μg/ml in PBS) for 1 min at RT. Samples were examined with a Leica TCS SP11 confocal microscope by use of a 530-nm band-pass filter for FITC detection and a 620-nm band-pass filter for the propidium iodide stain under a 100× objective lens. Color images were generated and analyzed with Leica confocal software, version 2.5.

Electron microscopy. Sf-21 cells (2×10^6) were infected with wild-type (wt) or recombinants of Ac*M*NPV at an MOI of 10. At 48 h postinfection (hpi), the infected cells were fixed in their culture flasks with 0.2% glutaraldehyde and 4% paraformaldehyde for 10 min on ice, centrifuged in 2-ml Eppendorf tubes, and fixed again for a further 50 min on ice. The cell pellets were washed three times in cold PBS and infused with 2.3 M sucrose in PBS at 4°C from between 8 h to overnight. Pieces of pellet were then mounted in fresh sucrose solution on aluminum pins (Leica) and plunge frozen into liquid nitrogen. Eighty-nanometer cryosections were cut on a Leica FCS Ultracut T with a dry diamond knife, collected onto plastic loops containing 2.3 M sucrose in PBS, and transferred to Formvar-carbon-coated glow-discharged 200-hexagonal-mesh copper-palladium

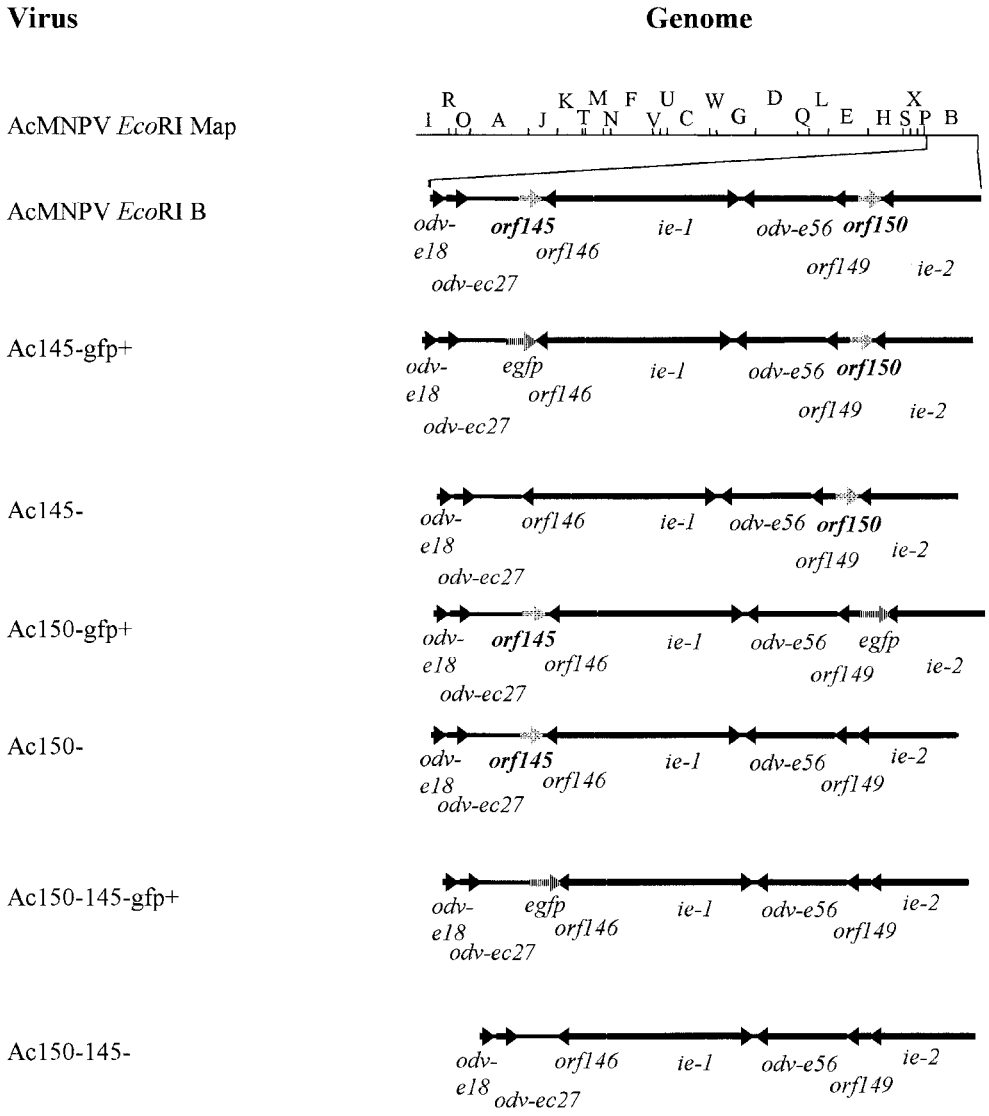

FIG. 1. Schematic representation of Ac*M*NPV genome and Ac145$^-$ and Ac150$^-$ deletion mutants. The black arrows show the location and orientation of ORFs in the Ac*M*NPV EcoRI B region where *orf145* and *orf150* are located. The gray arrows represent the location and orientation of *orf145* and *orf150*. The hatched arrows represent the location and orientation of the marker gene *egfp*.

grids (Agar Scientific) for immunogold labeling at RT on clean strips of Parafilm. Cryosections were blocked with 0.02 M glycine in PBS and 10% fetal bovine serum (FBS) in PBS for 10 min each, incubated in rabbit primary antibodies (anti-Ac145 and anti-Ac150) used at a 1:150 dilution in 10% FBS for 1 h, rinsed in PBS three times, followed by incubation in 10-nm protein A-gold beads (23) in 10% FBS for 30 min, quickly rinsed in PBS three times and distilled water six times, contrasted with 2% uranyl acetate in 0.2% methyl cellulose on ice for 10 min, picked up on loops, and air dried. The grids were viewed on a Philips CM100 transmission electron microscope.

Construction and identification of knockout mutant viruses. Transfer vector plasmids were constructed to generate Ac*M*NPV recombinants lacking either or both *orf145* and *orf150* genes by homologous recombination in infected insect cells. In the first instance, a plasmid was constructed by cloning the *Drosophila* heat shock 70 promoter in the SacII and BamHI sites of pBluescript II SK (+) (pBSHSP70). A second plasmid (pBSHS70-EGFP) was constructed to encode the *egfp* reporter gene (Clontech) downstream of the HSP70 promoter in the HindIII and EcoRI sites of pBSHSP70. The regions flanking *orf145* and *orf150* were subsequently PCR amplified (see below) and cloned upstream or downstream of the hsp70-*egfp* region.

The *orf145*-flanking ORFs (*odv-ec27* and *orf146*) (Fig. 1) and their control regions were kept intact as follows. Using oligonucleotide primers 145UF and 145DR (Table 1) the 1,066 nucleotides (nt) upstream of the *orf145* ATG (−1,066 to −1) were PCR amplified along with the region located at +6 to +14; this latter sequence corresponds to the putative poly(A) signal for the overlapping *orf146*. The 1,075-nt PCR-amplified DNA was cloned in the SacI and SacII sites of pBSHSP70-EGFP to create pBSHSP70-EGFP-145U. To amplify the region downstream of *orf145* but maintain the flanking *orf146* intact, which is in an opposite transcriptional orientation to *orf145*, an 834-nt region was PCR amplified from nt 256 of *orf145* with the primers 145DF and 145DR (Table 1). This region, which is inclusive of the 3′-terminal 32 nt of *orf145*, was cloned into the EcoRI and ApaI sites of pBSHSP70-EGFP-145U plasmid to create pEGFP+145−.

The *orf150*-flanking ORFs (*orf149* and *ie2*) (Fig. 1) and their control regions were kept intact as follows. To maintain the putative polyadenylation site of *ie2* intact, a 1,019-nt *orf150* downstream region was PCR amplified from nt +287 of *orf150* with primers 150DF and 150DR (Table 1). This region, which is inclusive of the 3′-terminal 15 nt of *orf150* was cloned into the EcoRI and KpnI sites of the pBSHSP70-EGFP plasmid to create pBSHSP70-EGFP-150D. The 877 nt upstream of the *orf150* ATG were PCR amplified along with the region up to +104 from the ATG with the 150UF and 150UR primers. The 981-nt PCR-amplified DNA fragment was cloned into the SacI and SacII sites of pBSHSP70-EGFP-150D to create pEGFP+150−.

Both pEGFP+145− and pEGFP+150− were further cloned to remove the

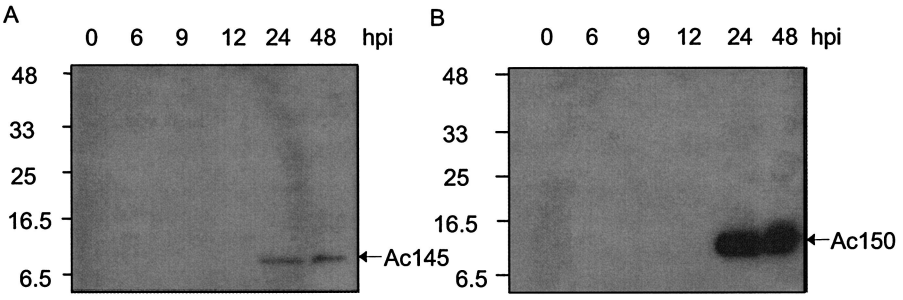

FIG. 2. Western blot analyses of Ac145 and Ac150 protein expression during time course infections of Sf-21 cells with wt Ac*M*NPV. (A) Cell lysates from Sf-21 cells infected with wt Ac*M*NPV were prepared at the indicated times postinfection, subjected to Western blot analysis, and probed with anti-Ac145 serum. (B) The cell lysates described for panel A were probed with anti-Ac150 serum.

reporter gene *egfp*, to produce transfer vectors for clean deletion viruses. The HSP70-EGFP fragment was removed by digestion of both pEGFP+145− and pEGFP+150− with SacII and EcoRI and blunt-ending the sites with T4 DNA polymerase before religating to create p145− and p150−.

The plasmids used for the creation of revertant viruses were prepared by PCR amplifying the *orf145* and *orf150* regions with the 145UF and 145DR primers and the 150UF and 150DR primers, respectively. A 2,157-bp DNA fragment of *orf145* (nt −1,066 to +1091) was cloned in the SacI and ApaI sites of pBluescript SK(−) to create p145rev. A 2,182-bp DNA fragment of *orf150* (nt −877 to +1305) was cloned in the SacI and KpnI sites of pBluescript II SK(+) to create p150rev.

Recombinant baculoviruses were constructed bearing deletions of *orf145* and *orf150* as follows. Viral DNA from Ac*M*NPV strain L1 was cotransfected with either plasmid pEGFP+145− or pEGFP+150−. These cotransfections allowed for the selection of viruses that encoded enhanced green fluorescent protein (EGFP) in place of either *orf145* or *orf150*. Recombinant viruses (Ac145$^-$ GFP$^+$ and Ac150$^-$ GFP$^+$) were selected based on the presence of EGFP-expressing plaques. The marker gene *egfp* was then removed by cotransfection of either Ac145$^-$ GFP$^+$ viral DNA with plasmid p145− or Ac150$^-$ GFP$^+$ viral DNA with plasmid p150−. Single deletion recombinant viruses (Ac145$^-$ and Ac150$^-$) were selected through purification of EGFP-negative plaques. To ensure that any effects observed in the single deletion mutants were caused only by the deletion of *orf145* or *orf150*, revertant viruses were also constructed. For this purpose, the deleted gene was reintroduced through cotransfections of either Ac145$^-$ GFP$^+$ viral DNA with plasmid p145rev or Ac150$^-$ GFP$^+$ viral DNA with plasmid p150rev. Revertant viruses (Ac145rev and Ac150rev) were selected through plaque purification of EGFP-negative plaques.

An Ac145 and Ac150 double deletion mutant virus was selected after cotransfection of Ac150$^-$ viral DNA with plasmid pEGFP+145−. The recombinant Ac150$^-$ Ac145$^-$ GFP$^+$ was selected based on the presence of EGFP-expressing plaques. The marker gene EGFP was then removed by cotransfection of Ac150$^-$ Ac145$^-$ GFP$^+$ viral DNA with plasmid p145− and the final double deletion mutant, Ac150$^-$ Ac145$^-$, was selected through plaque purification of EGFP-negative plaques. A partial revertant virus, where *orf145* was placed back into Ac150$^-$ Ac145$^-$, was prepared by cotransfection of Ac150$^-$ Ac145$^-$ GFP$^+$ viral DNA with plasmid p145rev to create Ac150$^-$145rev. The Ac150$^-$145rev virus was selected by plaque purification of EGFP-negative plaques.

To obtain all of the recombinant viruses, Sf-21 cells, at a density of 2×10^6 cells/60-mm-diameter dish, were cotransfected with 1 μg of viral DNA and 2 μg of transfer vector plasmid DNA by using the DOTAP liposomal transfection kit (Roche) as described by the manufacturer. All recombinant viruses were plaque purified between three to five times as previously described (18). The selected viral recombinants were amplified to passage 3, and the presence or absence of *orf145* and *orf150* genes in these recombinants was confirmed through restriction enzyme analysis of viral DNA and Western blot analysis of gene products from Sf-21 infected cell extracts.

Bioassays. Occlusion bodies (OBs) were purified from 5×10^4 Sf-21 cells, infected at an MOI of 10, with wt Ac*M*NPV or the EGFP-negative recombinant viruses described above. The OBs were harvested at 3 days postinfection, purified as previously described (18), and then fed to third instar *T. ni* larvae. OBs resulting from these in vivo infections were purified for use in bioassays. The LC_{50} (concentration of OBs required to reach 50% larval mortality), LD_{50} (number of PFU required to reach 50% mortality), and LT_{50} (mean time until death) were determined in neonates of *T. ni* or *H. virescens* larvae as previously described (10) by droplet feeding assays. *T. ni* or *H. virescens* larvae were fed a solution containing Ac*M*NPV wt, Ac145$^-$, Ac145rev, Ac150$^-$, Ac150rev, or Ac150$^-$145rev virus in concentrations ranging from 4×10^4 to 4×10^6 OBs/ml. Ac150$^-$ Ac145$^-$ virus concentrations fed to *T. ni* and *H. virescens* ranged from 4×10^4 to 1×10^7 and from 4×10^5 to 1×10^7 OBs/ml, respectively. Larvae were reared at 27°C in darkness. Mortality was recorded on a daily basis, although only those deaths after 3 days postinfection were counted as baculovirus related, and total mortality was recorded at 10 days postingestion. From 10 to 37 larvae were used per treatment group, and experiments were repeated between 4 to 7 times. The LC_{50} data were calculated with PoloPC (21), and LT_{50} values were calculated with ViStat (11). SigmaStat (SPSS, Inc.) was used to compare mean LC_{50}s with a two-way analysis of variance (ANOVA) which compared the virus LC_{50}s to one another and examined experiment-to-experiment variation. Where the ANOVA *P* value was significant (<0.05), pairwise comparisons were analyzed by the Holm-Sidak test.

The LD_{50} of budded viruses (BVs) was determined with fourth instar *H. virescens* larvae by hemocoelic injection by previously described methods (18), with different doses ranging from 0.01 to 7.8 PFU of BV that was produced and for which titers were determined in Sf-21 cells from either Ac*M*NPV wt or Ac150$^-$ Ac145$^-$ double deletion mutant viruses, diluted in TC100 medium (GIBCO) supplemented with antibiotics and antimycotics (Sigma). From 18 to 26 insects were injected per virus dose or with TC100 medium alone as a control (1 μl/insect). Mortality was recorded on a daily basis, and total mortality was recorded at day 7 postinjection. Experiments were repeated four times. The LD_{50} and LT_{50} were calculated as described above.

RESULTS

Expression kinetics and subcellular localization of the Ac*M*NPV ORF145 and ORF150 proteins. The anti-Ac145 serum and the anti-Ac150 serum each detected a single protein upon Western blot analysis of Ac*M*NPV-infected Sf-21 cell lysates (Fig. 2), although the band corresponding to Ac150 was quite diffuse (Fig. 2B). The putative Ac145 protein migrated as a smaller-molecular-mass protein than the putative Ac150 protein, both of which migrated between 8 to 11 kDa, which corresponded well to predicted proteins of 77 and 99 amino acids for each of the genes, respectively. Despite the fact that both proteins encode cysteine repeat domains with homology to each other (6), no antigenic cross-reactivity was detected between the two antisera. Both proteins were detected from 24 h through to very late times postinfection in Ac*M*NPV-infected Sf-21 cells (Fig. 2).

Western blot analyses indicated that cell lysates but not the extracellular media (data not shown) contained the Ac145 and Ac150 proteins, despite the presence of N-terminal hydrophobic sequences consistent with membrane transit signals (6). Immunofluorescence microcopy showed that Ac145 and Ac150 protein expression could be detected from 12 to 48 hpi, with the highest expression levels for both proteins occurring be-

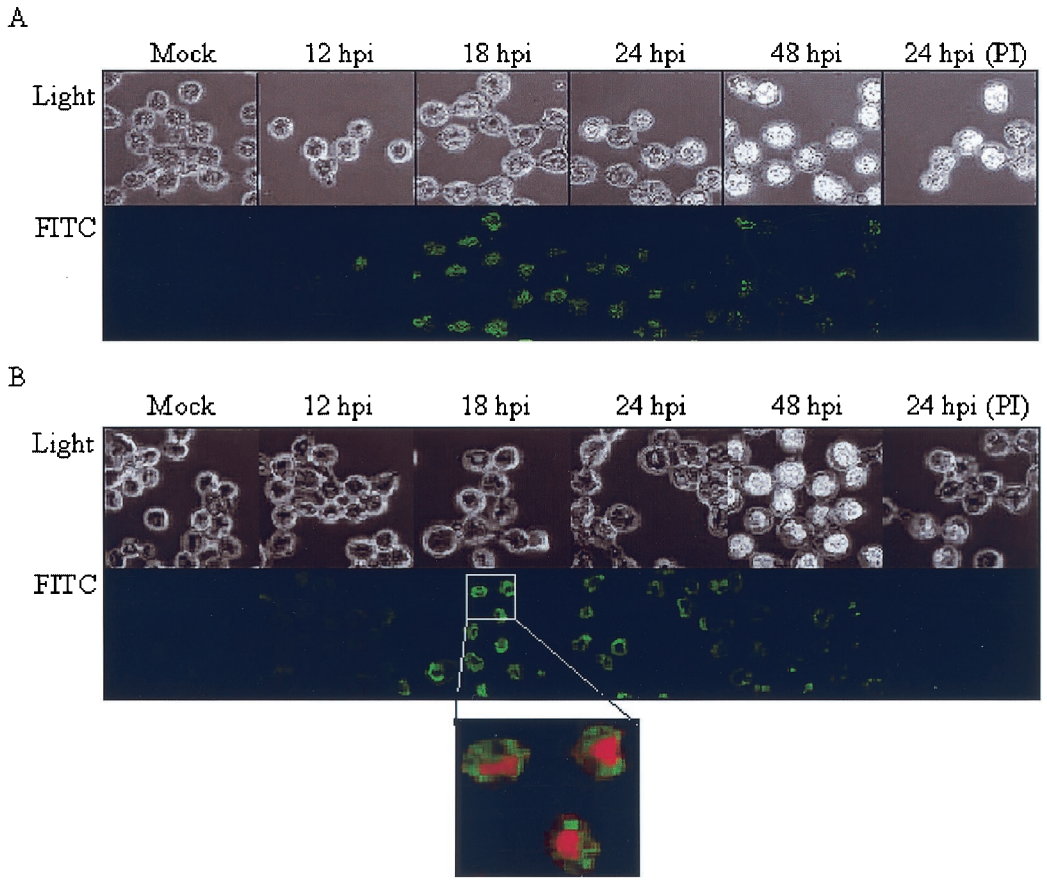

FIG. 3. Immunofluorescence analysis of Ac145 and Ac150 protein expression in Sf-21 cells infected with wt Ac*M*NPV at various times postinfection. (A) Sf-21 cells infected with wt Ac*M*NPV were fixed at indicated hours postinfection, probed with anti-Ac145 serum or preimmune serum (PI), and then probed with anti-rabbit secondary antibody conjugated with FITC. Cells were visualized by light and fluorescence microscopy (upper and lower rows, respectively). (B) The Sf-21 cells described for panel A were probed with anti-Ac150 sera or preimmune sera (PI) and then probed with the FITC-conjugated secondary antibody. The localization of nuclear DNA was determined by labeling the cells with propidium iodide (magnified panel).

tween 18 and 24 hpi (Fig. 3). Additionally, the localization of both proteins to infected nuclei was supported by comparison of the fluorescence patterns with that of propidium iodide staining and light microscope images of the cell (Fig. 3B, inset). Furthermore, at 18 and 24 hpi, the localization of these proteins in the infected cells appeared to coincide with regions of developing OBs within the nuclei when composite images were produced (data not shown). To determine whether Ac145 and Ac150 were associated with OBs, purified Ac*M*NPV OBs were analyzed by Western blot analysis and a small amount of Ac145 protein (Fig. 4A, lane 2) and relatively more Ac150 protein were detected with immune sera (Fig. 4B, lane 6) but not with preimmune sera (data not shown). Additionally, we isolated BV from infected-cell media, purified it from a sucrose step gradient, and subjected the BV to Western blot analysis (Fig. 4). Purified BV also showed the presence of Ac145- and Ac150-specific proteins with the immune antisera (Fig. 4A and B, lanes 4 and 8, respectively) but not with preimmune antisera (data not shown). Polyhedrin, the major constituent protein of OBs, was not detected with cross-reactive antibodies to polyhedrin (data not shown), indicating that there was no contamination of the BV fraction of the sucrose gradient with OBs. To ensure that roughly equal numbers of nucleocapsids from BV and ODV had been loaded per sample, the detection of a nucleocapsid structural protein, VP1054, was monitored (Fig. 4C) with anti-VP1054 serum (17). Interestingly, while the anti-Ac150 polyclonal antisera detected what appeared to be a protein doublet when samples were taken from BV (Fig. 4B, lane 8), OBs showed a single cross-reactive band of an intermediate molecular mass compared to the doublet seen for BV when examined by Western blot analysis (Fig. 4B, lane 6). Purified OBs from a baculovirus lacking both Ac145 and Ac150 ($Ac150^-$ $Ac145^-$, described below) and BV from $Ac150^-$ $Ac145^-$-infected-cell media were analyzed by Western blot analysis and found not to contain either of the Ac145 and Ac150 proteins (Fig. 4, lanes 1, 3, 5, and 7), as expected.

To further examine the localization of Ac145 and Ac150 with regard to developing OBs, immunogold labeling and transmission electron microscopy (TEM) of cryosections of Ac*M*NPV-infected Sf-21 cells at 48 hpi were performed. Preimmune sera from rabbits showed low cross-reactivity to either cellular or baculovirus structures such as OBs and virogenic stroma (Fig. 5A and C). Ac145 and Ac150 were both detected, as visualized by the presence of gold particles, in association

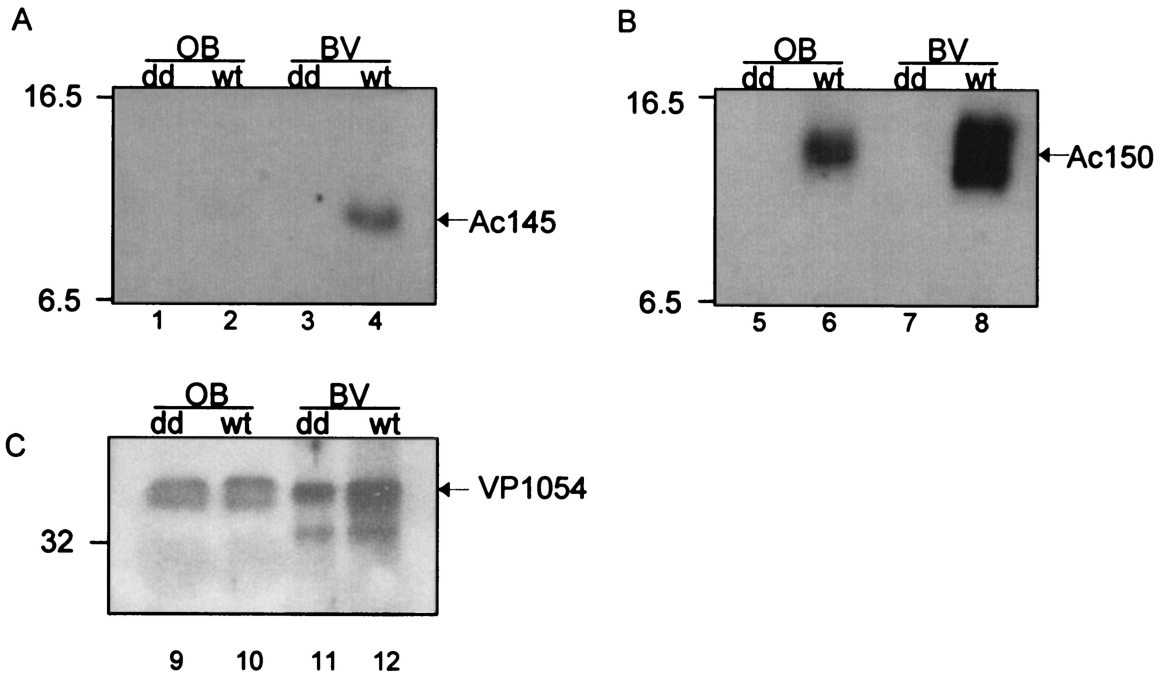

FIG. 4. Western blot analysis of Ac145 and Ac150 proteins in purified OBs and BV from wt Ac*M*NPV and Ac150$^-$ Ac145$^-$ (dd) virus. Purified OBs and BV from wt Ac*M*NPV and Ac150$^-$ Ac145$^-$ viral infections were subjected to Western blot analysis and probed with anti-Ac145 serum (A), anti-Ac150 serum (B), or antiserum for the baculovirus structural protein VP1054 (loading control) (C). Molecular mass markers in kilodaltons are indicated to the left of the panels.

with enveloped bundles of nucleocapsids within OBs (Fig. 5B and D) as well as with nucleocapsids in the process of maturation and occlusion (Fig. 5B and D). Sf-21 cells infected with recombinant viruses (described below) with deletions of Ac145 (Ac145$^-$), Ac150 (Ac150$^-$), or both genes (Ac150$^-$ Ac145$^-$) were examined for differences in the infected cell phenotypes compared to wt virus infection. Neither of the deleted proteins were detected by immunogold labeling in the respective deletion mutant-infected cells (Fig. 5E and G), but the localization of Ac145 in Ac150$^-$ mutant-infected cells (Fig. 5H) or Ac150 in Ac145$^-$ mutant-infected cells (Fig. 5F) was similar to their localization in wt infected cells. Ac150$^-$ Ac145$^-$ mutant-infected cells were also examined, and there was no immunogold labeling with anti-Ac145 antiserum, as expected, and the resulting OBs were morphologically similar to wt OBs (Fig. 5I).

Construction of recombinant viruses with deletions of ORF145 and ORF150. A series of Ac*M*NPV recombinant viruses were constructed, isolated, and purified to test the effects of knocking out *orf145*, *orf150*, or both genes simultaneously, on the growth and infectivity of these viruses (Fig. 1). Recombinants were first constructed where each gene was separately replaced with the *egfp* marker gene, which allowed for positive selection of the recombinant viruses by visualization of green fluorescent protein (GFP) expression. To be certain that any phenotypes associated with these recombinant viruses were due to the knockout of the selected viral gene rather than the expression of the GFP marker protein, *egfp* was subsequently removed through homologous recombination with transfer vectors containing either Ac145 or Ac150 flanking sequences, but lacking *egfp*, to give the recombinant viruses Ac145$^-$ and Ac150$^-$. To create a double knockout of both viral genes, the Ac150$^-$ recombinant virus was subjected to replacement of Ac145 with *egfp* to create the Ac150$^-$ Ac145$^-$ GFP$^+$ virus, which could be selected by production of GFP upon infection. Again to discount any GFP-related effects, a recombinant virus was produced by using the same strategy described above for replacing *egfp* to create a double knockout alone (Ac150$^-$ Ac145$^-$). Finally, to ensure that any phenotypes observed were not due to other unintentional mutations incurred during construction of these recombinant viruses, revertant viruses were made whereby the wt *orf145* gene was inserted back into the recombinant viruses Ac145$^-$ GFP$^+$ and Ac150$^-$ Ac145$^-$ GFP$^+$ and the wt *orf150* gene was inserted in the Ac150$^-$ GFP$^+$ virus. These revertant viruses, Ac145rev, Ac150$^-$145rev, and Ac150rev were selected for by the loss of GFP expression.

All of the recombinant viruses replicated in Sf-21 cells and produced similar titers of progeny virus (data not shown). To further verify that *orf145* and *orf150* were successfully deleted in these viruses, Western blot analysis was performed on infected Sf-21 cell lysates with Ac145-specific (Fig. 6A) and Ac150-specific (Fig. 6B) antibodies. These experiments showed that removal of the appropriate coding sequence resulted in a loss of the corresponding protein production and that the deletion of either gene did not affect the expression level of the other (Fig. 6A and B).

Bioassay analysis. We wanted to investigate the effects of deletion of these genes on the viral infection process. Therefore, neonate *T. ni* or *H. virescens* larvae were fed various doses of OBs purified from *T. ni* larvae infected with wt Ac*M*NPV, single deletion mutant virus Ac145$^-$ or Ac150$^-$, double deletion mutant Ac150$^-$ Ac145$^-$, full revertant virus Ac145rev or Ac150rev, or partial revertant virus Ac150$^-$145rev. The neo-

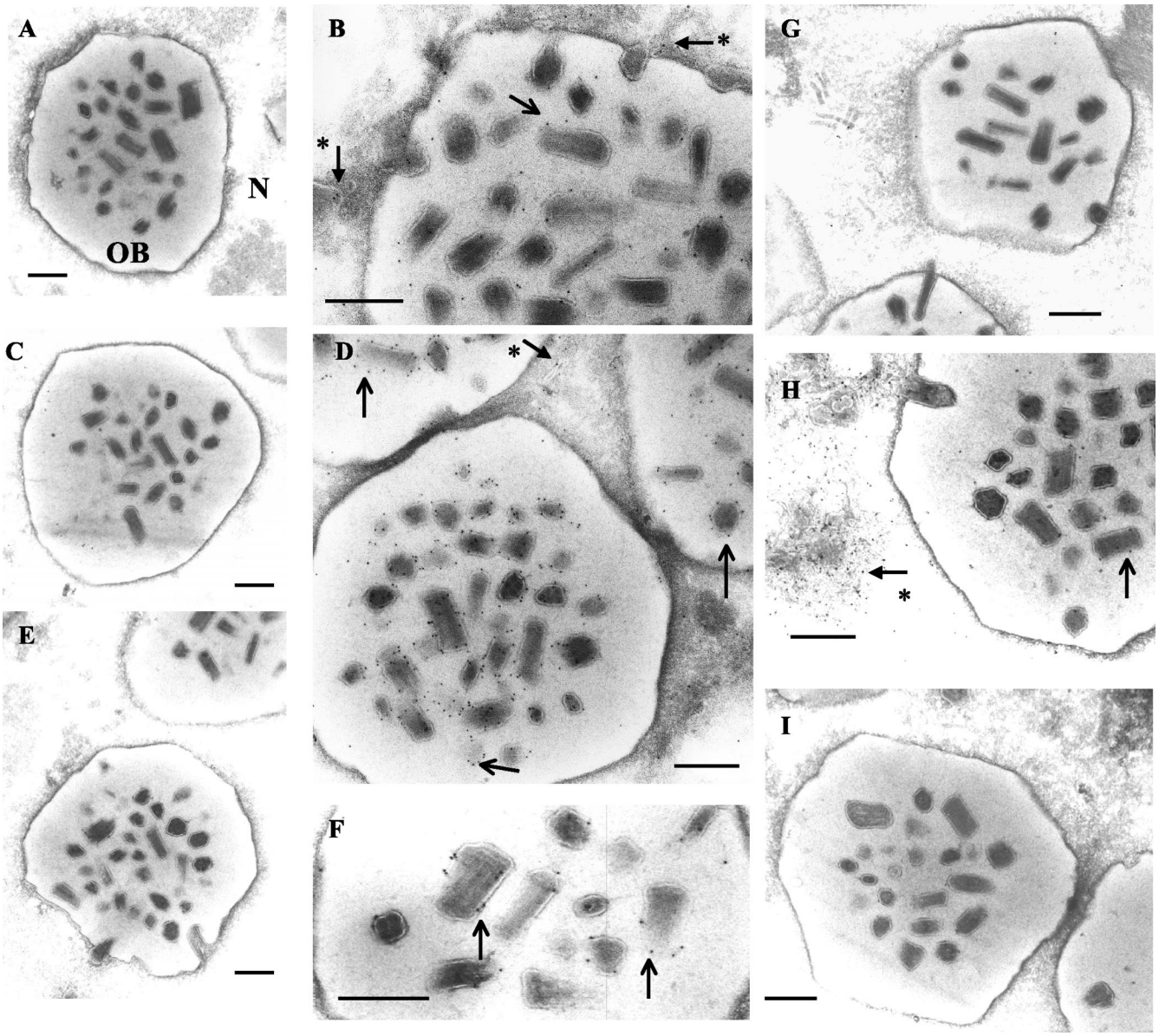

FIG. 5. TEM and immunogold labeling of Ac145 and Ac150 expression in wt Ac*M*NPV or deletion mutant-infected Sf-21 cells. Sf-21 cells were infected with wt Ac*M*NPV (A to D), a virus with a deletion of Ac145 (E and F), a virus with a deletion of Ac150 (G and H), or a virus with deletions of both Ac145 and Ac150 (I). Grids for TEM were incubated with anti-Ac145 (B, E, H, and I), its preimmune serum (A), anti-Ac150 (D, F, and G), or its preimmune serum (C). Plain arrows indicate gold particles associated with enveloped bundles of nucleocapsids within OBs, and arrows with an asterisk indicate those associated with developing nucleocapsids with the nuclei of infected cells. N, nucleus. Bars, 400 nm.

natal feeding was carried out per os via droplet feeding, and mortality was scored from 4 to 10 days postinfection.

The LC_{50} of neonate *H. virescens* larvae was determined for each virus (Fig. 7, upper panel). Deletion of either the Ac145 or Ac150 gene on its own compared to its revertant virus (Ac145$^-$ versus Ac145rev or Ac150$^-$ versus Ac150rev) or wt Ac*M*NPV was not significantly different, implying that the presence or absence of each single deletion did not significantly alter the dose-mortality response for the larvae. Deletion of both genes simultaneously (Ac150$^-$ Ac145$^-$) within a recombinant virus significantly reduced its potency compared to wt Ac*M*NPV (Fig. 7, upper panel). The drop in infectivity compared to wt Ac*M*NPV was 15.7-, 25.4-, 43.1-, and 72.5-fold in each of 4 experiments, which gives an average of an ~39-fold decrease. The partial revertant virus for the double deletion virus (Ac150$^-$145rev) does return to potency levels comparable to the Ac150$^-$ virus, as expected. Comparison of virus LC_{50}s over all the experiments was also measured, and no significant experiment-to-experiment variability was found (*P* value = 0.226). Assessing the time-mortality (LT_{50}) response to *H. virescens* larvae for these viruses showed that there were no significant differences between virus treatment groups as to when the infected larvae died (Table 2).

To test each of these viruses in another host, dose-mortality experiments were performed with neonate larvae of *T. ni* (Fig. 7, lower panel). In this host, recombinant virus with a deletion

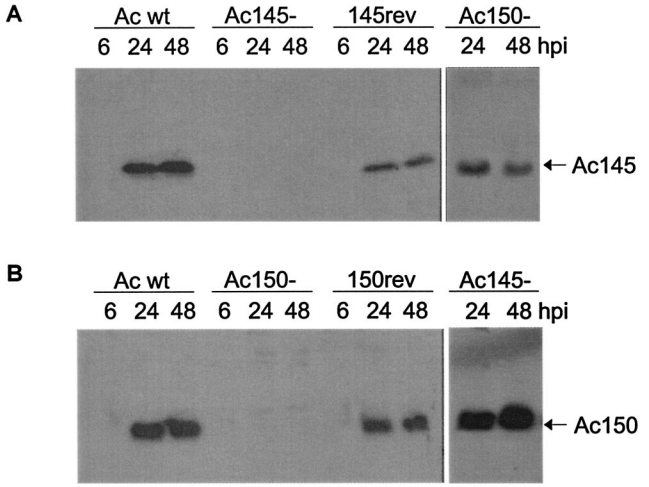

FIG. 6. Western blot analysis of Ac145 and Ac150 expression in Sf-21 cells infected with wt Ac*M*NPV (Ac wt), deletion mutant viruses Ac145$^-$ or Ac150$^-$, or their revertant viruses. (A) Cell lysates from Sf-21 cells infected with wt Ac*M*NPV, Ac145$^-$, a revertant virus (145rev), or Ac150$^-$ were prepared at indicated hours postinfection, subjected to Western blot analysis, and probed with anti-Ac145 serum. (B) Cell lysates from time course infections with wt Ac*M*NPV, Ac150$^-$, a revertant virus (150rev), or Ac145$^-$ used for Western blot analysis with anti-Ac150 serum.

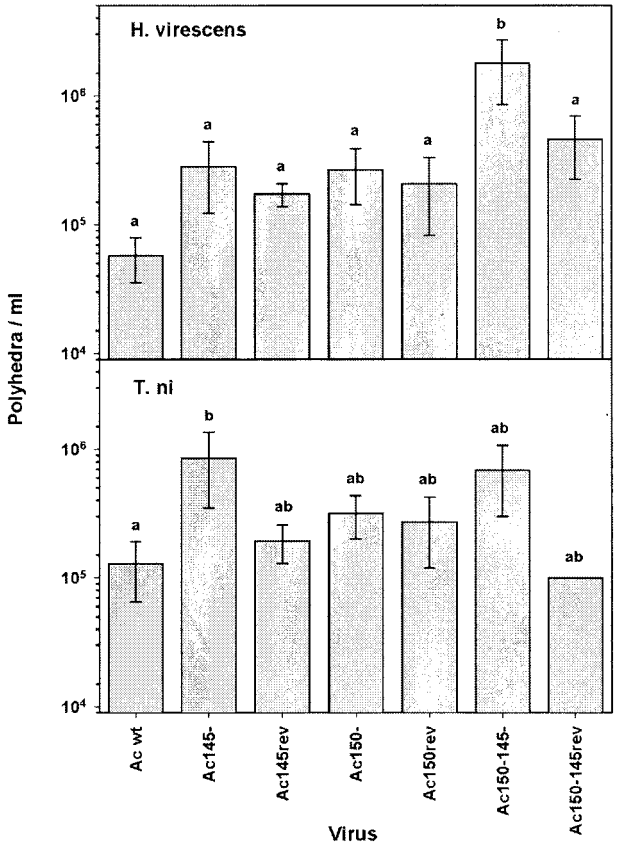

FIG. 7. Mean LC_{50}s for oral infectivity bioassays of *H. virescens* and *T. ni* with recombinant viruses or wt Ac*M*NPV. Median LC_{50}s with standard deviations, shown on individual bars, are presented for both *H. virescens* and *T. ni*. Within each host, viruses with different letters (a versus b) have significantly different mean LC_{50}s ($P < 0.05$, two-way ANOVA, Holm-Sidak method) in pairwise comparisons between viruses.

of Ac145 had a small but significantly higher LC_{50} than wt Ac*M*NPV, whereas the Ac150$^-$ recombinant virus did not have significantly different LC_{50}s compared to wt Ac*M*NPV. The Ac150$^-$ Ac145$^-$ double deletion recombinant virus mean LC_{50} was not significantly different from any of the viruses tested in this host. Taken together, this implies that deleting Ac145 alone causes a small drop in infectivity (2.2-, 4-, 7.9-, and 11-fold in each experiment with an average of an ~6-fold decrease compared to wt Ac*M*NPV), which is not additionally affected by a loss of Ac150. Comparison of LC_{50}s over all experiments did not show significant experiment-to-experiment variability (P value = 0.355). Time-mortality relationships for each of the viruses were also studied for infections of *T. ni*, but this parameter was similar among all the recombinant viruses and wt Ac*M*NPV (data not shown).

We then set up experiments to test whether the drop in the LC_{50} of the Ac150$^-$ Ac145$^-$ virus, relative to that of wt Ac*M*NPV seen for *H. virescens*, was due to less successful establishment of primary infection of midgut cells or to a problem with the systemic spread of secondary infection. BV derived from wt Ac*M*NPV and Ac150$^-$ Ac145$^-$ virus infections of Sf-21 cells were injected directly into the hemocoel of fourth instar *H. virescens*, thereby bypassing the primary infection of midgut cells. The dosage-mortality and time-mortality responses (Tables 3 and 4) were similar for both viruses, therefore indicating that the primary midgut infection and not the secondary infection was compromised in the Ac150$^-$ Ac145$^-$ virus infection of *H. virescens*.

DISCUSSION

At least 18 baculoviruses have been shown to encode homologues of the 11K gene of HaEPV. Some baculoviruses, such as Ac*M*NPV, encode one copy of each 11K subtype, *orf145* and *orf150*, while others encode multiple copies of the 11K gene of either type 145 or type 150 or both (6). We first characterized the expression of both gene products, Ac145 and Ac150, in Ac*M*NPV-infected Sf-21 cells and found that in accordance with the presence of baculovirus late transcription start sites (16) they are both expressed late in infection and remain detectable through 96 hpi. The predicted molecular mass of the 77-amino-acid Ac145 is 8.8 kDa while that of the 99-amino-acid Ac150 is 11.2 kDa, which was consistent with the migra-

TABLE 2. Time-mortality response of neonate *H. virescens* larvae infected per os by droplet feeding with wt Ac*M*NPV and various Ac*M*NPV deletion or revertant mutants of ORFs 145 and 150

Virus	LT_{50} (day) (mean ± SE)	Slope (mean ± SE)	% Mortality
Ac wt[a]	4.3 ± 0.2	17.6 ± 5.1	66.7
Ac145$^-$	4.7 ± 0.3	10.2 ± 2.9	66.7
Ac145rev	4.6 ± 0.2	18.1 ± 5.0	66.7
Ac150$^-$	4.7 ± 0.2	10.3 ± 2.7	77.8
Ac150rev	4.6 ± 0.2	19.9 ± 5.4	60.9
Ac150$^-$145$^-$	4.8 ± 0.2	12.0 ± 3.0	71.4
Ac150$^-$145rev	4.3 ± 0.3	7.0 ± 2.0	81.0

[a] Ac, Ac*M*NPV.

TABLE 3. Dose-mortality response of fourth instar *H. virescens* larvae injected with BV from wt Ac*M*NPV and an Ac*M*NPV with ORFs 145 and 150 knocked out

Virus	LD_{50} (PFU)	95% Fiducial limit		Slope (mean ± SE)	Hetero-geneity	Fold vs Ac wt[b]
		Lower	Upper			
Ac wt[a]	0.17	0.02	0.60	0.6 ± 0.2	0.7	NA[c]
Ac150$^-$145$^-$	0.14	0.02	0.48	0.8 ± 0.2	0.4	0.8

[a] Ac, Ac*M*NPV.
[b] Difference versus wt Ac*M*NPV.
[c] NA, not applicable.

tion rates obtained by Western blot analysis of infected whole-cell lysates. The intracellular localization of both Ac145 and Ac150 was determined by immunofluorescent confocal microscopy to be nuclear, and the signal could sometimes be seen as a ring at the edge of the nucleus, an area corresponding to the formation of BVs and OBs. Then at later time points (48 hpi) when the OBs are formed, the FITC signal seemed to decrease in intensity, even though the Western blot analysis of cell lysates showed the levels of both Ac145 and Ac150 in the cells rose slightly between 24 and 48 hpi (Fig. 2).

TEM coupled with immunogold labeling of Ac145 and Ac150 within sections of infected cells at 48 hpi supported the confocal microscopy data that showed these proteins to be localized within infected cell nuclei. The TEM experiments indicated a difference in the relative distribution of the Ac145 and Ac150 proteins within wt-infected cells. Some immunogold labeling for Ac145 was found in association with enveloped bundles of virions within the developing OBs, but a greater amount of labeling was seen within the nucleus in areas of nucleocapsid assembly and maturation (Fig. 5B and H). In contrast, immunogold labeling for Ac150 showed that most of the protein was found in association with occluded virions at this time of infection, with slightly less labeling seen for developing nucleocapsids (Fig. 5D and F). Taken together, these data showed that both Ac145 and Ac150 are part of wt Ac*M*NPV OBs that are ingested by caterpillar hosts, thereby supporting the hypothesis that these proteins are important for infection of the host via the oral route. Western blot analysis of purified OBs and BV from wt-infected cells in culture showed that both Ac145 and Ac150 are also present in BV (Fig. 4). In agreement with the TEM data, Ac145 was found at quite low levels by Western blot of purified OBs, with most of the protein found in association with BV. Purified BV and OBs both showed incorporation of Ac150, with BV-associated protein migrating as a doublet and OB-associated protein migrating as a single band of intermediate size (Fig. 4). This could explain the rather diffuse but single band seen from whole-cell lysates, which would contain all three forms of Ac150 migrating closely together (Fig. 2). To be certain that these migrational differences for Ac150 are not an artifact of analyzing quite small proteins by SDS-PAGE, further analysis would need to be done to show that some form of differential processing of Ac150 has occurred to produce variant proteins that migrate at slightly different rates by SDS-PAGE.

The combination of the presence of Ac145 and Ac150 in OBs, along with the putative chitin-binding motif in each protein would suggest that they are involved in the primary infection in the midgut of host caterpillars. We used an in vitro chitin-binding assay (data not shown) (22) to test whether Ac145 and/or Ac150 is able to bind to chitin, but these results were negative. Multiple conditions were tested in vitro that attempted to mimic the midgut environment (e.g., a pH range up to 10.5 or the presence of midgut juice), all of which gave negative chitin-binding results (data not shown), therefore we cannot determine at this point whether Ac145 and Ac150 do bind to chitin sheets present in the peritrophic matrix or perhaps interact with other host proteins or structures. Other peritrophin-like proteins (PL) are associated with the trachea of *Ctenocephalides felis* (cat flea) and the *Drosophila melanogaster* embryo (3, 7) as well as in the Malpighian tubules, hindgut, and rectum of *C. felis* (7). In addition to its location to a tissue that does not contain chitin, the PL1 protein of *C. felis* was also found to be negative for chitin-binding activity (7). These results support the previous hypothesis (3) that some PL proteins might not interact with the PM but could have functions that are nutrient and gas exchange related.

Recombinant viruses were produced for a deletion of the majority of the coding regions for Ac145, Ac150, or both, taking care not to perturb either the coding regions or flanking signals for expression of neighboring ORFs. Deletion of Ac145 and Ac150, either separately or within the same virus, did not change the morphology of infected cells or developing OBs (Fig. 5E to I and data not shown). The infectivity of the OBs from the Ac150$^-$ single deletion mutant virus was similar to that of wt Ac*M*NPV in both *T. ni* and *H. virescens* neonates (Fig. 7). OBs from the Ac145$^-$ single deletion mutant virus were as infectious as wt Ac*M*NPV OBs in *H. virescens* but were less infectious than wt Ac*M*NPV OBs to *T. ni* larvae (Fig. 7), indicating that Ac145 is more important to infection of *T. ni* caterpillars than *H. virescens* caterpillars. Despite the fact that deletion of either gene singly did not have a significant affect on infectivity for *H. virescens* larvae, infectivity of the OBs from the double deletion mutant (Ac150$^-$ Ac145$^-$) when compared to the infectivity of wt Ac*M*NPV OBs was decreased by 39-fold (Fig. 7). These data indicate that Ac145 and Ac150 probably have similar or overlapping functions in the midgut infectivity of *H. virescens*. This dramatic reduction in infectivity with Ac150$^-$ Ac145$^-$ was not seen for *T. ni*, the double deletion mutant virus had similar infectivity to the Ac145$^-$ single deletion virus for this host. None of the recombinant viruses showed a difference from wt Ac*M*NPV in terms of their time-mortality relationships within either host caterpillar (Table 2 and data not shown).

Finally, BV from the double deletion mutant showed the same infectivity as wt BV for *H. virescens* by intrahemocoelic injection (Tables 3 and 4), demonstrating that neither Ac145 nor Ac150 is required for Ac*M*NPV secondary spreading

TABLE 4. Time-mortality response of fourth instar *H. virescens* larvae injected with BV from wt and knockout Ac*M*NPV

Virus	LT_{50} (day) (mean ± SE)	Slope (mean ± SE)	% Mortality
Ac wt[a]	4.8 ± 0.3	9.2 ± 2.4	60.0
Ac150$^-$145$^-$	4.7 ± 0.3	10.2 ± 2.8	60.0

[a] Ac, Ac*M*NPV.

through the *H. virescens* caterpillar or to cause mortality. This was surprising given the fact that both the Ac145 and Ac150 proteins had been found as a component of wt Ac*M*NPV BV.

Ac150 has recently been demonstrated by DNA microarray analysis to be differentially expressed in two different cell lines (31). In agreement with our protein immunodetection analysis, the *orf150* gene was shown to be expressed from a late time postinfection in Sf9 cells. However, the authors found that *orf150* was poorly expressed in the *T. ni* High-Five cell line compared to the *S. frugiperda* Sf9 cell line, suggesting differential requirements for Ac150 in different host cells. The fact that neither Ac145 nor Ac150 was required for infectivity in *T. ni* neonate caterpillars is consistent with the finding the *orf150* was poorly expressed in a *T. ni* cell line. Although we did not test the infectivity of our mutants for *S. frugiperda* caterpillars, we would hypothesize that Ac150, at least in combination with Ac145, would offer a competitive advantage for Ac*M*NPV infection in this species.

Intriguing questions as to the individual roles of each of the 11K-like proteins remain. The presence of two 11K homologues in Ac*M*NPV begs the question as to whether the presence of multiple copies of the 11K genes in a single virus, for example, *Xestia c-nigrum* granulovirus (XcGV) (NC 00233) (9), which has 5 copies, might not support an increased infectivity in specific hosts and viral competitiveness in the environment. In addition, XcGV also has multiple copies of enhancins, which were also shown to support OB infectivity of LdMNPV in *L. dispar* larvae (19). Based upon the importance of having either the Ac145 or Ac150 protein during primary infection of *H. virescens*, it is interesting that most NPVs do not encode enhancins while all lepidopteran-infecting NPVs encode 11K homologues. It would be of great interest to more precisely determine the in vivo role of Ac145 and Ac150 to Ac*M*NPV infection of the *H. virescens* midgut. It would also be valuable to determine what role, if any, these proteins have in the BV. Although mortalities for *H. virescens* larvae injected with BV from wt Ac*M*NPV or Ac150$^-$ Ac145$^-$ virus were similar in this assay, more subtle phenotypic differences such as total virus yield from these infected insects or the tissue distribution of infection in cadavers may be different between wt and the recombinant viruses and should be examined carefully in the future.

ACKNOWLEDGMENTS

This work was supported by grant no. 28/P11541 from the Biotechnology and Biological Sciences Research Council (BBSRC) of the United Kingdom.

Mention of trade names or commercial products in this article is solely for the purpose of providing scientific information and does not imply recommendation or endorsement by the U.S. Department of Agriculture.

We thank David Dall for initial input on this project and Syngenta for the gift of *H. virescens* eggs.

REFERENCES

1. **Aguinaldo, A. M. A., J. M. Turbeville, L. S. Linford, M. C. Rivera, J. R. Garey, R. A. Raff, and J. A. Lake.** 1997. Evidence of a clade of nematodes, arthropods and other moulting animals. Nature **387:**489–493.
2. **Ayres, M. D., S. C. Howard, J. Kuzio, M. Lopez-Ferber, and R. D. Possee.** 1994. The complete DNA sequence of *Autographa californica* nuclear polyhedrosis virus. Virology **202:**586–605.
3. **Barry, M. K., A. A. Triplett, and A. C. Christensen.** 1999. A peritrophin-like protein expressed in the embryonic tracheae of *Drosophila melanogaster.* Insect Biochem. Mol. Biol. **29:**319–327.
4. **Bell, R. A., C. D. Owens, M. Shapiro, and J. R. Tardif.** 1981. Mass rearing and virus production: development of mass-rearing technology, p. 599–655. *In* C. C. Doane and M. L. McManus (ed.), The gypsy moth: research toward integrated pest management. U.S. Forest Service Technical Bulletin 1584. U.S. Forest Service, Washington, D.C.
5. **Cory, J. S., R. S. Hails, and S. M. Sait.** 1997. Baculovirus ecology, p. 301–339. *In* L. K. Miller (ed.), The baculoviruses. Plenum Press, New York, N.Y.
6. **Dall, D., T. Luque, and D. O'Reilly.** 2001. Insect-virus relationships: sifting by informatics. Bioessays **23:**184–193.
7. **Gaines, P. J., S. J. Walmsley, and N. Wisnewski.** 2003. Cloning and characterization of five cDNAs encoding peritrophin-A domains from the cat flea, *Ctenocephalides felis.* Insect Biochem. Mol. Biol. **33:**1061–1073.
8. **Gallo, L. G., B. G. Corsaro, P. R. Hughes, and R. R. Granados.** 1991. In vivo enhancement of baculovirus infection by the viral enhancing factor of a granulosis virus of the cabbage looper *Trichoplusia ni* (Lepidoptera: Noctuidae). J. Invertebr. Pathol. **58:**203–210.
9. **Hayakawa, T., R. Ko, K. Okano, S. I. Seong, C. Goto, and S. Maeda.** 1999. Sequence analysis of the Xestia c-nigrum granulovirus genome. Virology **262:**277–297.
10. **Hughes, P. R., N. A. M. van Beek, and H. A. Wood.** 1986. A modified droplet feeding method for rapid assay of *Bacillus thuringiensis* and baculoviruses in noctuid larvae. J. Invertebr. Pathol. **48:**187–192.
11. **Hughes, P. R.** 1990. ViStat: statistical package for the analysis of baculovirus bioassay data. Boyce Thompson Institute at Cornell University, Ithaca, N.Y.
12. **Kuzio, J., M. N. Pearson, S. H. Harwood, C. J. Funk, J. T. Evans, J. M. Slavicek, and G. Rohrmann.** 1999. Sequence and analysis of the genome of a baculovirus pathogenic for *Lymantria dispar.* Virology **253:**17–34.
13. **Lepore, L. S., P. R. Roelvink, and R. R. Granados.** 1996. Enhancin, the granulosis virus protein that facilitates nucleopolyhedrovirus (NPV) infections, is a metalloprotease. J. Invertebr. Pathol. **68:**131–140.
14. **Li, Q., C. Donly, L. Li, L. G. Willis, D. A. Theilmann, and M. Erlandson.** 2002. Sequence and organization of the *Mamestra configurata* nucleopolyhedrovirus genome. Virology **294:**106–121.
15. **Mayo, M. A., and C. R. Pringle.** 1998. Virus taxonomy—1997. J. Gen. Virol. **79:**649–657.
16. **Miller, L. K.** 1997. The baculoviruses. Plenum Press, New York, N.Y.
17. **Olszewski, J., and L. K. Miller.** 1997. Identification and characterization of a baculovirus structural protein, VP1054, required for nucleocapsid formation. J. Virol. **71:**5040–5050.
18. **O'Reilly, D. R., L. K. Miller, and V. A. Luckow.** 1992. Baculovirus expression vectors: a laboratory manual. W. H. Freeman and Company, New York, N.Y.
19. **Popham, H. J. R., D. S. Bishoff, and J. M. Slavicek.** 2001. Both *Lymantria dispar* nucleopolyhedrovirus *enhancin* genes contribute to viral potency. J. Virol. **75:**8639–8648.
20. **Regev, A., M. Keller, N. Strizhov, B. Sneh, E. Prudovsky, I. Chet, I. Ginzberg, Z. Koncz-Kalman, C. Koncz, J. Schell, and A. Zilberstein.** 1996. Synergistic activity of a Bacillus thuringiensis delta-endotoxin and a bacterial endochitinase against *Spodoptera littoralis* larvae. Appl. Environ. Microbiol. **62:**3581–3586.
21. **Robertson, J. L., and M. K. Preisler.** 1992. Pesticide bioassays with arthropods. CRC Press, Boca Raton, Fla.
22. **Shen, Z., and M. Jacobs-Lorena.** 1998. A type I peritrophic matrix protein from the malaria vector *Anopheles gambiae* binds to chitin. J. Biol. Chem. **273:**17665–17670.
23. **Slot, J. W., and H. J. Geuze.** 1985. A new method of preparing gold probes for multiple-labeling cytochemistry. Eur. J. Cell Biol. **38:**87–93.
24. **Tanada, Y., and H. Kaya.** 1993. Insect pathology. Academic Press, San Diego, Calif.
25. **Tellam, R.** 1996. Biology of the insect midgut, p. 86–108. *In* M. J. Lehane and P. F. Billingsley (ed.), The insect midgut. Chapman & Hall, London, United Kingdom.
26. **Tellam, R. L., G. Wijffels, and P. Willadsen.** 1999. Peritrophic membrane proteins. Insect Biochem. Mol. Biol. **29:**87–101.
27. **Volkman, L. E., and B. A. Keddie.** 1990. Nuclear polyhedrosis virus pathogenesis. Semin. Virol. **1:**249–256.
28. **Wang, P., and R. R. Granados.** 1997. An intestinal mucin is the target substrate for a baculovirus enhancin. Proc. Natl. Acad. Sci. USA **94:**6977–6982.
29. **Wang, P., and R. R. Granados.** 2000. Calcofluor disrupts the midgut defense system in insects. Insect Biochem. Mol. Biol. **30:**135–143.
30. **Wood, H. A., and R. R. Granados.** 1991. Genetically engineered baculoviruses as agents for pest control. Annu. Rev. Microbiol. **45:**69–87.
31. **Yamagishi, J., R. Isobe, T. Takebuchi, and H. Bando.** 2003. DNA microarrays of baculovirus genomes: differential expression of viral genes in two susceptible insect cell lines. Arch. Virol. **148:**587–597.